Catalysis Today 148 (2009) 174–178

Contents lists available at ScienceDirect

Catalysis Today

journal homepage: www.elsevier.com/locate/cattod

Effects of pore structure of post-treated TS-1 on phenol hydroxylation

Shang-Tien Tsai [a], Pei-Yu Chao [a], Tseng-Chang Tsai [a,*], Ikai Wang [b], Xinxu Liu [c], Xin-Wen Guo [c]

[a] Department of Applied Chemistry, National University of Kaohsiung, 700 Kaohsiung University Rd., Nan-Tzdu Dist., Kaohsiung 811, Taiwan
[b] Department of Chemical Engineering, National Tsing Hua University, 300 Hsinchu, Taiwan
[c] State Key Lab of Fine Chemicals, Dalian University of Technology, 116012 Dalian, China

ARTICLE INFO

Article history:
Available online 28 March 2009

Keywords:
Post-treatment
TS-1
Phenol hydroxylation
Mesoporous zeolite

ABSTRACT

The present study reports the effects of crystal size of TS-1 (micrometer sized umTS1 and nanometer sized nmTS1) and the post-treatment (TPAOH and NaOH treatment) on the porous structure and the catalytic performances of TS-1 in phenol hydroxylation. TPAOH post-treatment generates hollow crystal and increases the surface area of umTS1 without changing its pore structure. In contrast, NaOH treatment selectively dissolves framework silica to form mesopore and modify microporous structure through which hierarchical material is constructed with agglomerated crystals. The umTS1 sample gives a much lower conversion and lower selectivity of dihydroxylbenzenes (DHB) than the nmTS1 sample. Its activity can be greatly improved by TPAOH post-treatment exhibiting a comparable catalytic activity and DHB selectivity with the nmTS1 sample. Furthermore, successive post-treatment by TPAOH following with NaOH can generate micropores larger than the pore size of TS-1. The higher titanium content and faster diffusivity associated with the successive post-treatment significantly improve the catalytic performance of TS-1.

1. Introduction

EniChem Corporation successfully developed a new phenol hydroxylation process in 1986 by using TS-1 catalyst and hydrogen peroxide oxidant in replacement of the traditional Brichima process (homogeneous system using Fe^{2+}/Co^{2+} catalyst) for the production of hydroquinone (HQ) and catechol (CT). Since then, the catalysis of titanium containing molecular sieves has been extended to many other oxidation reactions [1]. The TS-1 catalysis involves a five membered ring intermediate generated by reacting titanium peroxy species (Ti–OOH) with the hydroxyl group of solvent molecules [2]. Formation of the bulky five membered ring intermediate reduces the pore volume of TS-1 and, thus, imposes remarkable diffusion resistance of substrates upon TS-1 [3]. As a result, the catalytic performance of TS-1 is strongly affected by the molecular size of substrate and oxidant, nature of solvent, crystal size, pore structure and hydrophobicity [4,5]. Effect of crystal size on phenol hydroxylation is still not clear. Wilkenhöner et al. reported that smaller crystallite TS-1 has higher catalytic activity [4]. Kerton et al. reported that oxidation of crotyl alcohol does not require TS-1 structure, but phenol hydroxylation is catalyzed only by crystalline TS-1. Phenol hydroxylation occurs only on the exterior surface of large TS-1 crystallites, with smaller crystallites of TS-1, the reaction could occur on the exterior of the crystallites or at sites within the porous structure [5]. Generally speaking, in titanium silicate and mesoporous Fe-HMS [6], water is a better solvent. Furthermore, from catalyst stability viewpoint, the loss of Ti through leaching during oxidation using peroxide is of great concerned particularly Ti-beta [7]. Some catalysts such as Ti-beta [8,9] and Fe-HMS [6] have different hydrophilic/hydrophobic properties and thus different product distribution from TS-1.

While TS-1 is limited to the application of those substrates and oxidants smaller than its pore opening of 5.4 Å, many new types of catalysts were studied in the catalysis for large molecules such as mesoporous Fe-HMS [6], superconductor mixed oxides Cu–Bi–V–O complex [10], mesoporous titanosilicates [11], vanadium-substituted phosphomolybdate [12], Fe-containing pillared clays [13], Fe/KIT-polystyrene composite [14], and metalloporphyrin complexes [15].

Although titanium silicates with periodic mesoporous structure can possess improved accessibility of active sites and the diffusion of substrate molecules inside the pore system, mesoporous titanium silicates were found to exhibit much lower intrinsic activity than TS-1 [16].

Introducing mesoporosity into zeolite can improve the diffusivity of zeolite [17]. Cejka and Mintova recently reviewed the preparation and catalysis of micro/mesoporous composite and hierarchical material [18,19]. Hierarchical material can be prepared either by direct synthesis, post-chemical treatment or formation of zeolite monoliths [20,21]. Among various post-treatment methods, Groen

* Corresponding author.
E-mail address: tctsai@nuk.edu.tw (T.-C. Tsai).

0920-5861/$ – see front matter © 2009 Elsevier B.V. All rights reserved.
doi:10.1016/j.cattod.2009.02.018

et al. reported that desilication of MFI zeolite by alkaline post-treatment can create mesopores more effectively than dealumination procedure does [22]. Tuel and coworkers reported that TS-1 catalytic activity can be improved by TPAOH post-treatment [23]. Recently, we found that the catalytic performance of TPAOH treated TS-1 can be significantly improved by alkaline post-treatment [24]. The present paper studies the effect of different post-treatments on the pore structure of TS-1 and its catalytic performance in phenol hydroxylation.

2. Experimental

Nanometer sized TS-1, denoted as nmTS1, was synthesized hydrothermally at 443 K for 12–24 h from a gel mixture of SiO_2:TiO_2:TPAOH:IPA:H_2O = 1:0.02:0.20–0.35:1.0:25–50 using TEOS as silica precursor and *t*-butyl orthotitanate as titanium precursor following the procedure reported by Guo et al. [25–27]. On the other hand, micrometer sized TS-1, denoted as umTS1, was synthesized from the gel at the composition the same gel composition as nmTS1 but using tetrapropylammonium bromide (TPABr) as template and triethylamine as organic base, colloidal silica as silica source and $TiCl_4$ as titanium precursor. Those TS-1 samples were calcined in flowing air stream at 813 K for 8 h to remove organic template.

The parent umTS1 sample was post-treated with TPAOH solution of 0.15 mol/L hydrothermally at 443 K for 48 h, which was denoted as MT-umTS1; or with NaOH solution of various concentrations, represented as solution A (2×10^{-2} mol/L), B (4×10^{-4} mol/L) and C (2×10^{-3} mol/L), at 353 K for *x* minutes, denoted as NaXx-umTS1. Successive post-treatment was also conducted by treating first with TPAOH and then with NaOH solution, denoted as NaXx-MT-umTS1. Similarly, parent nmTS1 sample was post-treated to prepare MT-nmTS1, NaXx-nmTS1 and NaXx-MT-nmTS1. The NaOH treated samples were then ion exchanged with 1 mol/L NH_4NO_3 solution at 353 K for 6 h and finally calcined in air at 813 K for 8 h.

The structures of various TS-1 samples were determined with a Rigaku Multiflex X-ray diffractometer using Cu Kα radiation and their compositions were analyzed by PerkinElmer Optima 2100 DV inductive coupling plasma (ICP-AES) spectrometer. The surface area was determined by BET method using Micromeritics ASAP2020. Prior to the measurements, samples were degassed at 373 K for 1 h and at 623 K for 4 h at a pressure less than 1.4 Pa. Nitrogen adsorption was conducted at 77 K. The pore size distribution was calculated by the Barrett–Joyner–Halenda (BJH) method using the desorption branch of the isotherm. A temperature programmed desorption (TPD) of hexane isomers [28] was devised to determine the micropore structures of the parent and posted treated TS-1 samples. The experimental setup was a gas chromatography (GC) equipped with a flame ion detector (FID). A stainless steel (ss) tube packing with zeolite sample of 25 mg is used as the column of the GC. The column is heated to 573 K in nitrogen carrier gas flow for 3 h to desorb any adsorbed substances particularly water. Adsorption measurement was conducted in nitrogen flow by pulse injecting one hexane isomer at 308 K and atmospheric pressure until breakthrough as on-line observed with GC FID signal. Desorption was conducted first at 308 K for 30 min and then by raising oven temperature at a heating rate of 5 °C/min up to 573 K. The desorption capacity was measured from the FID peak area calibrated with a known volume of the hexane isomer.

Phenol hydroxylation reaction was conducted in a rotary reactor in batch mode using a reaction mixture with the composition of phenol:H_2O_2 = 3:1. Oxidation products were analyzed by an Agilent 5890 Gas Chromatography equipped with a FID detector using an OV-101 column. The molecular formula of reaction products were determined using Varian Star 3380 GC/MASS spectrometer equipped with TR-5MS column.

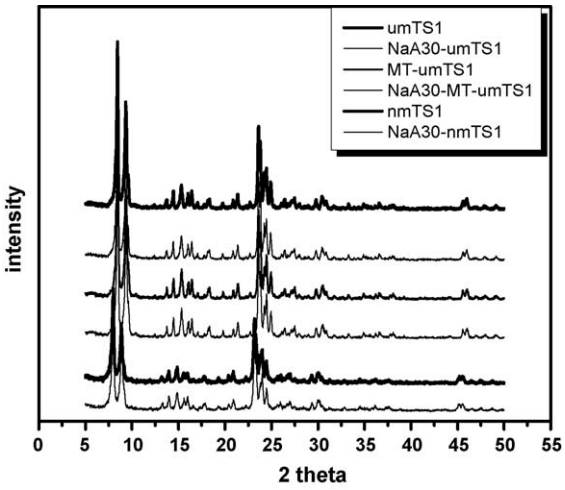

Fig. 1. X-ray diffraction patterns of the parent TS-1 and post-treated TS-1 sample.

3. Results and discussion

As shown in Fig. 1, all the X-ray diffraction patterns of the tested samples, including micrometer sized umTS1 and nanometer sized nmTS1 as well as the post-treated samples, possessed pure TS-1 phase. Therefore, post-treatment with TPAOH or NaOH at the stated conditions do not destroy MFI framework structure. The crystal size of the TS-1 sample determined with transmission electromicroscopy (TEM) was about 5 μm for the umTS1 sample and 50 nm for the nmTS1 sample. Micrometer sized TS-1 can be prepared with conventional method using TPABr as template and triethylamine as organic base [29]. On the other hand, nmTS-1 be prepared using organic base TPAOH as template [30].

The umTS1 and nmTS1 sample subject to TPAOH treatment kept the same crystal size but turned into hollow crystal in TPA-umTS1 sample. On the other hand, NaOH treatment form aggregates of nano-crystals. Cundy et al. reported that morphology of MFI crystal changes with NaOH solution treatment [31]. As shown in Table 1, both the parent umTS1 and MT-umTS1 have Ti content determined with ICP-AES as 4.0 wt.%. Similar effect was observed on the post-treated nmTS1 sample, showing unchanged Ti content of 3.5 and 3.7 wt.% in nmTS1 and MT-nmTS1, respectively. In contrast, NaOH post-treatment raises titanium content. The titanium content increases up to 5.2 and 4.2 wt.% respectively in the NaOH treated NaA30-umTS1 and NaA30-nmTS1 sample. On the other hand, the titanium content increases slightly in the successive treated sample first with TPAOH following with NaOH up to 4.2% in the NaA30-MT-umTS1 and 4.0 wt.% in the NaA30-MT-nmTS1. Therefore, TPAOH post-treatment can generate holes inside crystal without changing crystal composition. In contrast, alkaline treatment can dissolve silica and disintegrate crystal agglomerates.

Table 1
Textural properties of various TS-1 samples determined with nitrogen adsorption isotherm.

Sample	Ti (wt.%)	S_{BET} (m^2/g^{-1})	S_{meso} (m^2/g^{-1})	S_{micro} (m^2/g^{-1})	V_{meso} ($cm^3\ g^{-1}$)	Mesopore size (Å)
umTS1	4.0	404.5	131.4	273.1	0.10	47.2
MT-umTS1	4.0	425.2	150.9	274.2	0.13	44.9
NaA30-umTS1	5.2	346.6	110.5	236.1	0.19	22.4
NaA30-MT-umTS1	4.2	416.9	148.8	268.1	0.23	22.9
nmTS1	3.5	546.2	341.0	205.1	0.50	74.8
MT-nmTS1	3.7	423.8	261.1	162.7	0.31	69.6
NaA30-nmTS1	4.2	507.2	230.8	276.4	0.41	98.3
NaA30-MT-nmTS1	4.0	428.4	275.3	153.2	0.33	75.0

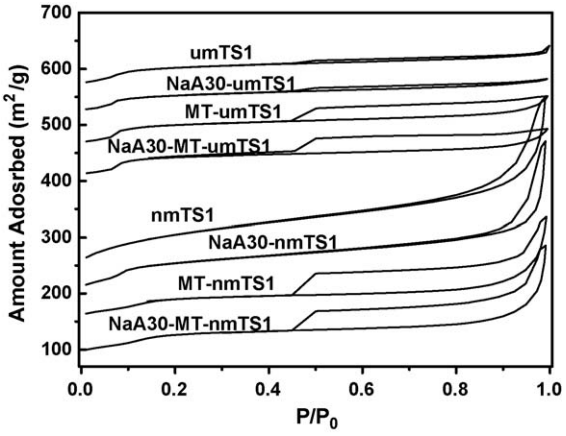

Fig. 2. Nitrogen adsorption and desorption isotherm.

The nitrogen adsorption and desorption isotherm of the studied samples are shown in Fig. 2. Both the TPAOH and NaOH treatment generate type IV isotherm with hysteresis loops of type H4 in the umTS1 and nmTS1, showing substantial mesopore formation in the post-treated TS-1 samples. The BET surface area and pore size distribution are summarized in Table 1. The nmTS1 sample possesses much larger BET surface area up to 546.2 m^2/g and mesopore volume at mesopore size of 74.8 Å which are higher than that of umTS1 sample. Subject to TPAOH post-treatment, the mesopore size of MT-mmTS1 and MT-nmTS1 both decrease slightly. Furthermore, the surface area of MT-nmTS1 increases slightly from 404.5 m^2/g up to 425.2 m^2/g but that of MT-nmTS1 decreases down to 423.8 m^2/g. On the other hand, by NaOH treatment, the pore size of umTS1 reduces but that of nmTS1 increases. The surface area and pore size of NaA30-MT-umTS1 reduced but that of NaA30-MT-nmTS1 increases. As discussed below, the micropore of umTS1 is reduced by NaOH treatment. The change of surface area associated with different post-treatments could be attributed to the change of morphology and silica defects associated with the leaching of silica and titanium. It was known that zeolite composition is not homogeneous in zeolite crystal [32]. The change of textural properties is specific to different parent TS-1 samples and treatment protocols. The dissolved silica in severe alkaline treatment could deposit on zeolite pore, making pore opening become narrower.

Micropore determination of hierarchical material with the traditional BET method becomes more complicated [33]. In this study, the micropore structures of various TS-1 samples were characterized by the temperature program desorption of hexane isomers, viz., n-hexane (nC_6), 2-methylpentane (2MP) and 2,2-dimethylbutane (DMB), as shown in Fig. 3(A) and (B). The desorption capacity of various hexane isomers can be used to measure the pore void volume accessible for different molecular cross sections [28]. Desorption temperature is getting higher as the interaction between adsorbate and TS-1 zeolite pore wall becomes stronger. Generally speaking, the desorption temperature increases with decreasing pore size decreases [28] or longer diffusion length. As shown in Table 2, the umTS1 has about the same desorption capacity as nmTS1 with the capacity of 11.87 and 5.95 wt.% for umTS1 in the sorption of nC_6 and 2MP and 11.0 and 5.83 wt.% for nmTS1 correspondingly. The nC_6 sorption appeared two desorption peaks and 2MP sorption gave one desorption peak. The desorption temperature of 2MP in umTS1 and nmTS1 was 471 and 433 K, respectively. The same desorption capacity with lower desorption temperature in nmTS1 than umTS1 clearly indicates faster diffusion by reducing crystal size.

Table 2
Temperature programmed desorption of hexane isomers.

Sample ID	n-C_6		(CH_3)–C_5		$(CH_3)_2C_4$	
	wt.%	T (K)	wt.%	T (K)	wt.%	T (K)
umTS1	11.87	420/488	5.95	471	0	–
MT-umTS1	13.31	383/448	6.68	434	0	–
NaA30-umTS1	10.80	430/511	5.45	452	0	–
NaA30-MT-umTS1	12.73	394/461	6.25	445	0	–
nmTS1	11.00	387/451	5.83	433	0	–
MT-nmTS1	10.09	371/436	4.94	415	0	–
NaA30-nmTS1	11.21	370/425	6.44	410	0	–
NaA30-MT-nmTS1	9.33	399/484	5.20	478	0.89	496

Subject to TPAOH treatment, the desorption capacity of MT-umTS1 increased significantly from 11.87 wt.% up to 13.31 wt.% with reducing desorption temperature from 488 K down to 448 K. On the other hand, NaOH treated NaA30-umTS1 shows a slight lower sorption capacity at even higher desorption temperature of nC_6, indicating a slight pore plugging with reduced pore opening. Similarly, NaA30-MT-umTS1 subject to NaOH treatment shows lower desorption capacity at higher desorption temperature. As discussed above, reduced mesopore size occurs is also was observed.

However, the nmTS1 shows reversed effects of post-treatment on its sorption properties. The MT-nmTS1 gives lower desorption capacity and desorption temperature. On the other hand, NaA30-nmTS1 gives higher desorption capacity appearing at lower desorption temperature, indicating enlarged pore opening with NaOH post-treatment. The successive post-treatment in NaA30-MT-umTS1 leads to lower desorption capacity at higher desorption

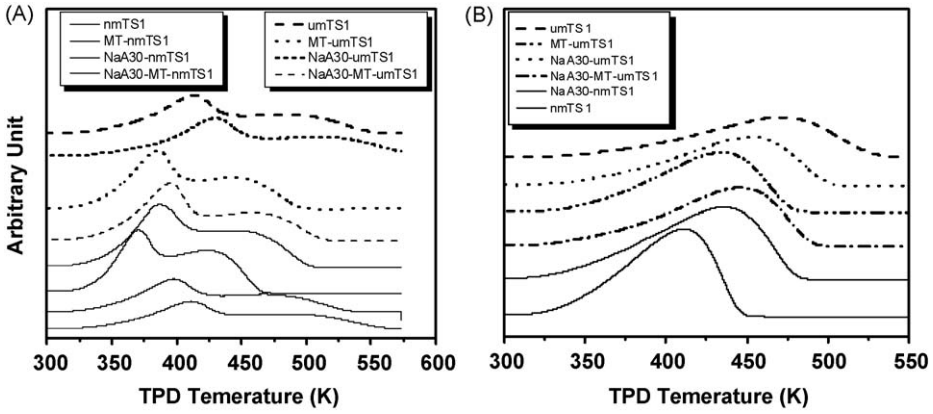

Fig. 3. Temperature programmed desorption of (A) n-hexane and (B) 2-methylpentane.

Table 3
Product selectivity of parent and post-treated umTS1 and nmTS1 sample at various substrate/oxidant ratio (solvent: acetone; rx. temperature: 333 K; rx. time: 6 h).

Catalyst ID	X (%)	S_R (%)	CT/HQ	Product distribution (%)			
				CT	HQ	BQ	OCHD
umTS1	1.6	65.5	6.7	56.99	8.48	4.16	30.37
MT-umTS1	14.6	94.3	1.1	48.95	45.32	0.09	5.64
NaA30-umTS1	5.0	82.3	3.2	62.58	19.68	1.56	16.18
NaA30-MT-umTS1	4.4	82.1	3.2	62.58	19.49	1.03	16.9
nmTS1	17.1	97.6	1.3	54.39	43.16	<0.01	2.44
MT-nmTS1	8.8	99.9	1.9	65.68	34.21	0	0.11
NaA30-nmTS1	11.3	93.2	1.2	50.44	42.74	0.03	6.79
NaA30-MT-nmTS1	18.0	99.7	1.6	60.88	38.77	0.01	0.34

temperature and more interestingly, significant sorption capacity of DMB. Presumably, the successive post-treatment protocol generates new micropores larger than 10-membered oxygen ring (10-MR).

To sum up, the NaOH treatment on umTS1 results in lower BET surface area and TPD capacity. In contrast, alkaline treatment on nmTS1 increases mesoporosity and microporosity. Our earlier study showed that the surface area of the alkaline hydroxide treated TS-1 decreases with increasing basicity in the order of LiOH < NaOH < KOH < CsOH [24]. The large micropores can be formed after treated with LiOH, NaOH and KOH solution. On the other hand, treatment with more basic CsOH solution leads to partially collapses of TS-1 structure with a much lower surface area.

The absorption band at 960 cm^{-1} in FT IR spectra represents the stretching mode of SiO_4 unit bonded to a Ti^{4+} ion as a useful probe of zeolitic framework titanium site [34]. All the studied samples exhibit the relative peak intensity at 960 cm^{-1}. Based on ICP-AES, XRD and IR spectra as discussed above, it is presumed that TPAOH treatment generates mesopores inside crystals without attacking the framework structure. On the other hand, the alkaline treatment can selectively leach out silica from zeolitic framework and create more porosity.

The catalytic performance of parent umTS1 and nmTS-1 and their post-treated samples is shown in Table 3. While the micro-sized umTS1 sample having higher Ti content gives very low conversion at only 1.6%, the nano-crystal nmTS1 sample has conversion of 17.1%. Furthermore, the umTS1 catalyzes a lower selectivity of dihydroxylbenzenes (DHB) with more side products benzoquinone (BQ), and 4-hydroxycyclohexa-2,5-dienone (OCHD) than the nmTS1 does. As indicated by the lower TPD temperature to have higher diffusion rate, the more active nmTS1 can be attributed to its nano-size morphology.

Moreover, the catalytic properties of TS-1 samples are affected significantly by various post-treatments. At comparable Ti content, the TPAOH post-treatment greatly enhances the conversion of micro-crystal TS-1 from 1.6% up to 14.6% but it deteriorates the catalytic activity of nano-crystal TS-1 from phenol conversion of 17.1% down to 8.8%. Interestingly, TPAOH treated MT-umTS1 has catalytic conversion of 14.6% which is only slightly lower than the conversion of 17.1% over the parent nmTS1 sample. As discussed above, TPAOH post-treatment upon umTS1 sample leads to higher BET surface area and desorption capacity of nC_6 and 2MP at lower desorption temperature of MT-umTS1 with comparably the same Ti content. Therefore, the improved catalytic performance of MT-umTS1 should be attributed to the modified textural property. Nevertheless, the effect of TPAOH treatment upon nmTS1 is reversed. Lower BET surface area and also lower TPD capacity of MT-nmTS1 results in worsened performance.

On the other hand, NaOH post-treatment selectively removes framework silica and increases the titanium content of the post-treated samples [24]. With the slight higher titanium content, the conversion of Na-umTS1 slightly increases. The NaOH treatment on nmTS1 results in lower BET surface area but a higher TPD capacity, implying the 10MR pore slightly enlarges after the post-treatment.

The effect of a sequential post-treatment first with TPAOH and then NaOH was studied on the micro-sized NaA30-MT-umTS1 and the nano-sized NaA30-MT-nmTS1 sample. For the micro-sized mnTS1, the conversion over the successive post-treatment NaA30-MT-umTS1 becomes poorer than the single TPAOH treated MT-umTS1. Most interestingly, as shown in the TPD capacity of DMB, the successive TPAOH and then NaOH treated nmTS1 generates a large pore greater than 10MR. Although lower surface area and TPD capacity of nC_6 and 2MP were observed, the successive post-treatment shows a synergistic effect in NaA30-MT-nmTS1 to give a higher conversion than the single post-treatment method and the parent nmTS1.

The effect of post-treatment on the surface area and pore structure varies with treatment condition and sample type. As shown in Table 4, post-treatment with very dilute NaOH solution at concentration of 4×10^{-4} M in NaC15-umTS1 can significantly enhance phenol conversion up to 13.6% giving HQ as the primary product at CT/HQ ratio down to 0.4. Treating with increasing concentration of NaOH solution, the improved phenol conversion of umTS1 by post-treatment diminishes along with increasing CT/HQ ratio. As shown in Table 5, successive post-treatment with NaOH even at very dilute NaOH solution at concentration of 4×10^{-4} M following TPAOH treatment still deteriorates phenol conversion. High selectivity of HQ was observed giving CT/HQ ratio down to 0.3, which is comparable with the dilute NaOH treated umTS1. The result indicates that product selectivity is affected by the textural properties of the TS-1 catalyst samples.

The CT/HQ ratio in phenol hydroxylation over most Ti-containing zeolite catalysts is within the range 0.5–1.3 and basically depends on the solvent and conversion. Two hypotheses have been proposed to explain CT/HQ product selectivity. According to the hypothesis of Tuel and Ben Taarit, steric hindrance of transition complex is favorable for the formation of *p*-isomer HQ, following by the isomerization of HQ into CT on the external surface of TS-1, thus increases the CT/HQ ratio [35]. Kerton et al. proposed that phenol oxidation occurs on the exterior crystallite surface or within the pores close to the surface of the crystallites [5]. On the other hand, Wilkenhöner et al. observed that CT/HQ ratio does not change after inactivation of external surface activity

Table 4
Effect of NaOH post-treatment conditions on the catalytic performances of NaOH treated umTS1 catalyst (solvent: acetone; rx. temperature: 333 K; rx. time: 6 h).

Catalyst ID	NaOH treatment		X (%)	S_R (%)	CT/HQ	Product distribution (%)			
	Concentration (M)	T (min)				CT	HQ	BQ	OCHD
umTS1	–	–	1.6	65.5	6.7	56.99	8.48	4.16	30.37
NaC15-umTS1	4×10^{-4}	15	13.6	69.2	0.4	21.13	48.01	0.57	30.29
NaB15-umTS1	2×10^{-3}	15	10.3	78.0	0.6	28.93	49.03	1.17	20.87
NaA15-umTS1	2×10^{-2}	15	7.1	88.1	0.9	42.43	45.63	1.33	10.61
NaA30-umTS1	2×10^{-2}	30	5.0	82.3	3.2	62.58	19.68	1.56	16.18

Table 5
Effect of successive NaOH post-treatment conditions on the catalytic performances of TPAOH treated MT-umTS1 catalyst (solvent: acetone; rx. temperature: 333 K; rx. time: 6 h).

Catalyst ID	NaOH treatment		X (%)	S_R (%)	CT/HQ	Product distribution (%)			
	Concentration (M)	T (min)				CT	HQ	BQ	OCHD
MT-umTS1	–	–	14.6	94.3	1.1	48.95	45.32	0.09	5.64
NaC15-MT-umTS1	4×10^{-4}	15	7.3	78.0	0.3	19.36	58.67	0	21.97
NaB15-MT-umTS1	2×10^{-3}	15	9.0	90.4	1.3	51.79	38.65	0.35	9.21
NaA30-MT-umTS1	2×10^{-2}	30	4.4	82.1	3.2	62.58	19.49	1.03	16.90

by consecutive chemical vapor deposition cycles. They concluded that catechol is formed inside the pore of TS-1 and external surface plays a key role in determining conversion and selectivity [4]. In addition, in comparison of TS-1 vs Al-free Ti-beta, smaller pore openings led to a decreased conversion with enhanced selectivity for HQ. On the other hand, Clerici et al. proposed that the intrinsic activity of titanium sites declines progressively with increasing pore diameter [36]. Phenol hydroxylation is controlled by diffusion [4,37]. Therefore, the effect of post-treatments on the catalytic performance of TS-1 catalyst can be resulted from the modification of textural properties and pore structure as well as titanium content. The nanometer sized nmTS1 has faster diffusion rate and thus much higher activity than the micrometer sized umTS1. By TPAOH post-treatment, the diffusivity in umTS1 can be improved by generating hollow crystal, showing catalytic performance comparable to the nmTS1. On the other hand, the diffusivity of NaOH treated nmTS1 changes with the formation of hierarchical TS-1 material by generating mesopores and modified microporous structures. Improved catalytic performance was observed in the hierarchical material NaA30-MT-nmTS1 by successive treatments of TPAOH and NaOH. The result demonstrates the catalytic potential of hierarchical zeolites in oxidation reactions.

4. Conclusion

The effect of post-treatment using TPAOH and NaOH on the porous structure of TS-1 and its effect on the catalytic performance of phenol hydroxylation were investigated. BET isotherm and temperature programmed desorption of hexane isomers were used to monitor the change of micropore structures with various post-treatments. It was found that TPAOH post-treatment on the micrometer crystallite TS-1 sample (umTS1) generates hollow crystals which increases sorption capacity and shortens diffusion pathways. In contrast, TPAOH treatment on nanometer sized TS1 (nmTS1) reduces surface area without modifying pore structure. On the other hand, NaOH treatment selectively dissolves framework silica, thus the modified nmTS1 sample has higher titanium content and mesopores with modified micropore. Interestingly, successive NaOH post-treatment following TPAOH treatment generates large micropores in nmTS1 capable for adsorption of 2,2-dimethylbutane, presumably greater than framework 10-MR pore. Presumably, TPAOH and NaOH post-treatment can increase the torturosity of porous system and expose Ti sites with increasing accessibility.

It was observed that pore structure of various TS-1 catalysts can significantly affect phenol conversion and reaction selectivity. Due to slower diffusion rate, the umTS1 gives a much lower conversion at only 1.6% and a lower selectivity of DHB than the nmTS1 at 17.1%. The catalytic performance of umTS1 can be greatly improved by TPAOH post-treatment showing a comparable catalytic activity and DHB selectivity with nmTS1. In contrast, catalyst performance of TPAOH treated MT-nmTS1 dwindles. The catalytic performance of MT-nmTS1 can be improved by successive NaOH post-treatment. The improved catalytic performance can be attributed to a higher titanium content and improved diffusivity by the generation of large micropores. In conclusion, alkaline treatment can generate mesopore with framework Ti intact, and improve the catalytic performance of TS-1.

Acknowledgement

We acknowledge the National Science Council of the Republic of China for financial support (NSC 96-2120-M-390-001).

References

[1] C. Perego, A. Carati, P. Ingallina, M.A. Mantegazza, G. Bellussi, Appl. Catal. A: Gen. 221 (2001) 63.
[2] G. Bellussi, A. Carati, M.G. Clerici, G. Maddinelli, R. Millini, J. Catal. 133 (1992) 220.
[3] P. Wu, T. Komatsu, T. Yashima, J. Phys. Chem. B 102 (1998) 9297.
[4] U. Wilkenhöner, G. Langhendries, F. van Laar, G.V. Baron, D.W. Gammon, P.A. Jacobs, E. van Steen, J. Catal. 203 (2001) 201.
[5] O.J. Kerton, P. McMorn, D. Bethell, F. King, F. Hancock, A. Burrows, C.J. Kiely, S. Ellwood, G. Hutchings, Phys. Chem. Chem. Phys. 7 (2005) 2671.
[6] H. Liu, G. Lu, Y. Guo, Y. Guo, J. Wang, Nanotechnology 17 (2006) 997.
[7] A. Carati, C. Flego, E. Previde-Massara, R. Millini, L. Carluccio, W.O. Parker Jr., G. Bellussi, Micropor. Mesopor. Mater. 30 (1999) 13.
[8] M.A. Camblor, M. Costantini, A. Corma, L. Gilbert, P. Esteve, A. Martinez, S. Valencia, J. Chem. Soc., Chem. Commun. (1996) 1339.
[9] T. Blasco, M.A. Camblor, A. Corma, P. Esteve, J.M. Guil, A. Martinez, J.A. Perdigon-Melon, S. Valencia, J. Phys. Chem. B 102 (1998) 75.
[10] J. Sun, X. Meng, Y. Shi, R. Wang, S. Feng, D. Jiang, R. Xu, F.S. Xiao, J. Catal. 193 (2000) 199.
[11] S.K. Mohapatra, F. Hussain, P. Selvam, Catal. Commun. 4 (2003) 57.
[12] J. Chen, S. Gao, J. Xu, Catal. Commun. 9 (2008) 728.
[13] S. Letaief, B. Casal, P. Aranda, M.A. Martin-Luengo, E. Ruiz-Hitzky, Appl. Clay Sci. 22 (2003) 263.
[14] A. Dubey, M. Choi, R. Ryoo, Green Chem. 8 (2006) 144.
[15] H.Q. Zeng, Q. Jiang, Y.F. Zhu, X.H. Yan, X.B. Liang, H.Y. Hu, Q. Liu, W.Y. Lin, C.C. Guo, J. Porphyr. Phthalocyan. 10 (2006) 96.
[16] K. Kulawik, G. Schulz-Ekloff, J. Rathouský, A. Zukal, J. Had, Collect. Czech. Chem. Commun. 60 (1995) 451.
[17] J.C. Groen, W. Zhu, S. Brouwer, S.J. Huynink, F. Kapteijn, J.A. Moulijn, J. Pérez-Ramirez, J. Am. Chem. Soc. 129 (2007) 355.
[18] J. Cejka, S. Mintova, Catal. Rev.-Sci. Eng. 49 (4) (2007) 457.
[19] S. Mintova, J. Cejka, Stud. Surf. Sci. Catal. 168 (2007) 301.
[20] S. van Donk, A.H. Janssen, J.H. Bitter, K.P. de Jong, Catal. Rev. 45 (2) (2003) 297.
[21] Y. Tao, H. Kanoh, L. Abrams, K. Kaneko, Chem. Rev. 106 (2006) 896.
[22] J.C. Groen, L.A.A. Peffer, J.A. Moulijn, J. Perez-Ramirez, Chem. Eur. J. 11 (2005) 4983.
[23] Y. Wang, M. Lin, A. Tuel, Micropor. Mesopor. Mater. 102 (2007) 80.
[24] P.Y. Chao, S.T. Tsai, T.C. Tsai, J. Mao, X.W. Guo, Top. Catal. 50 (1–2) (2009) 185.
[25] X.S. Wang, X.W. Guo, Catal. Today 51 (1999) 177.
[26] J.B. Mao, M. Liu, P. Li, Y. Liu, X.W. Guo, Acta Petrol Ei Sin. 24 (1) (2008) 57.
[27] G. Li, X.W. Guo, X.S. Wang, Q. Zhao, X.H. Bao, X.W. Han, L.W. Lin, Appl. Catal. A: Gen. 185 (1999) 11.
[28] P.Y. Chao, Y.Y. Chuang, G.H. Ho, S.H. Chuang, T.C. Tsai, C.Y. Lee, S.T. Tsai, J.F. Huang, J. Chem. Educ. 85 (11) (2008) 1558.
[29] M. Taramasso, G. Perego, B. Notari, US 4,410,501 (1983).
[30] A. Tuel, Zeolites 16 (2–3) (1996) 108.
[31] C.S. Cundy, M.S. Henty, R.J. Plaisted, Zeolites 15 (1995) 342.
[32] J. Dwyer, F.R. Fitchf, R. Machado, G. Qin, S.M. Smyth, J.C. Vickerman, J. Chem. Soc., Chem. Commun. (1981) 422.
[33] P. Kowalczyk, M. Jaroniec, K. Kaneko, A.P. Terzyk, P.A. Gauden, Langmuir 21 (2005) 10530.
[34] S. Klein, W.F. Maier, Angew. Chem. Int. Ed. 35 (1996) 2230.
[35] A. Tuel, Y. Ben Taarit, Appl. Catal. A 102 (1993) 69.
[36] M.G. Clerici, in: R.A. Sheldon, H. van Bekkum (Eds.), Fine Chemicals through Heterogeneous Catalysis, Wiley-VCH, Weinheim, 2001, p. 538.
[37] A.J.H.P. van der Pol, A.J. Verduyn, J.H.C. van Hooff, Appl. Catal. A: Gen. 92 (1992) 113.